



EM Wave Coupling Noise Modeling Based on Chebyshev Approximation and Exact Moment Formulation

Baohua Wang, Pinaki Mazumder

► To cite this version:

Baohua Wang, Pinaki Mazumder. EM Wave Coupling Noise Modeling Based on Chebyshev Approximation and Exact Moment Formulation. DATE'05, Mar 2005, Munich, Germany. pp.976-981. <hal-00181254>

HAL Id: hal-00181254

<https://hal.science/hal-00181254v1>

Submitted on 23 Oct 2007

HAL is a multi-disciplinary open access archive for the deposit and dissemination of scientific research documents, whether they are published or not. The documents may come from teaching and research institutions in France or abroad, or from public or private research centers.

L'archive ouverte pluridisciplinaire **HAL**, est destinée au dépôt et à la diffusion de documents scientifiques de niveau recherche, publiés ou non, émanant des établissements d'enseignement et de recherche français ou étrangers, des laboratoires publics ou privés.



HAL Authorization

EM Wave Coupling Noise Modeling Based on Chebyshev Approximation and Exact Moment Formulation

Baohua Wang and Pinaki Mazumder

Department of Electrical Engineering and Computer Science

University of Michigan, Ann Arbor, Michigan, 48109, USA

Email: {baohuaw, mazum}@eecs.umich.edu

Abstract

This paper presents a new mathematical approach to modeling EM wave coupling noise so that it can be easily integrated into chip-level noise analysis tools. The new method employs Chebyshev approximation technique to model the distributed sources arising in the Telegrapher's equations due to EM wave coupling. A uniform plane wave illumination metric is provided to determine the order of approximation. Closed-form formulas for the noise transfer functions' moments are derived. By utilizing the formulated moments, reduced order models can be efficiently obtained to generate the induced noise caused by EM wave illumination. The accuracy of the proposed method is verified by Hspice simulation.

1. Introduction

Signal integrity is of paramount importance for reliable operation of very deep submicron CMOS VLSI chips. Noise analysis is performed by designers to verify the stability and timing specifications of the chip [3], [7]. Previously, IR drop, Ldi/dt noise, coupling noise induced by signal switching were mainly considered [1], [11]. However, interconnect noises induced by external electromagnetic wave illumination must also be addressed. For example, PC board can carry high-frequency signals through the long metal wires. They often behave as antenna by illuminating the pins of the mounted VLSI chip by system-generated EM waves. The induced noise incident on the chip pins can propagate inside the chip to severely affect the signal integrity of the internal circuit. EM effect, therefore, can manifest itself, e.g. as timing failures, due to impairment of signal integrity.

The analysis of the EM wave coupling to long wires is traditionally based on full-wave field solvers or SPICE-like simulators [2], [9]. However, such type of approaches are generally unsuitable for chip-level noise analysis due to

their prohibitive computational costs. This paper presents a new approach to modeling the external EM wave coupling in signal traces between two circuit components, e.g., buffer/repeaters inside a chip, or I/O ports on PCB. The proposed approach efficiently generates the induced noise waveforms that should be used as noise sources into chip-level noise analysis flows to verify the signal integrity of the chip illuminated by external EM waves.

One difficulty in the modeling of EM wave coupling noise is the handling of distributed sources in the Telegrapher's equations describing EM wave coupling, since they correspond to an infinite number of lumped sources in the resultant equivalent TL (transmission line) circuit. To handle these sources, the proposed approach employs Chebyshev approximation technique because of its fast convergence and *minmax* property. After the order of approximation is determined by using the proposed uniform plane wave illumination metric, actual field values will be used for further computations. Therefore, the usual assumption of uniform plane wave illumination in analyzing EM wave coupling is not required any more.

Reduced order models (ROM's) are proposed in the paper to generate noise waveforms. ROM's have been derived for RC, RLC, TL circuits [6], [4], [10]. They either require efficient moment generation, which is, however, lacked for the TL circuit considering EM wave coupling, or do not provide closed-form representations. This paper presents closed-form representations of the transfer functions' moments for the used TL circuit. Therefore, ROM's can be quickly obtained to generate noise waveforms.

The rest of the paper is organized as follows. Section 2 introduces the modeling EM wave coupling with long interconnects, driver circuit model, and its noise transfer functions. Section 3 introduces the modeling of distributed sources using Chebyshev approximation, and the proposed uniform plane wave illumination metric to determine the order of approximation. Section 4 presents the derived closed-form moments' representations, and ROM's of noise transfer functions. Section 5 presents the experimental results.

2. EM Wave Coupling Noise Modeling

2.1. Telegrapher's Equations with EM Coupling

The behavior of the long interconnect (TL) being illuminated by EM waves, is governed by the Telegrapher's equations, with distributed source terms having been incorporated [5]. For a TL of length d and height h , locating in the $x-z$ plane given by $y=0$, with x axis as its longitudinal direction, the governing equations in s -domain, when the line is illuminated by EM wave, is written as:

$$\frac{d}{dx}V(s,x) + [R(x) + sL(x)]I(s,x) = V_f(s,x) \quad (1a)$$

$$\frac{d}{dx}I(s,x) + [G(x) + sC(x)]V(s,x) = I_f(s,x) \quad (1b)$$

$V_f(s,x)$ and $I_f(s,x)$ denote source terms describing the incident EM wave coupling. They are given as:

$$V_f(s,x) = [E_{x,0,h}^i(s) - E_{x,0,0}^i(s)] \cdot \mathbf{e}_x - \frac{\partial V_f^i(s,x)}{\partial x} \quad (2a)$$

$$I_f(s,x) = -[G(x) + sC(x)]V_f^i(s,x). \quad (2b)$$

$V_f^i(s,x)$ is the defined incident voltage, which is given, using the incident electric field E^i of the EM wave, as:

$$V_f^i(s,x) = \int_0^h E_{x,0,z}^i(s) \cdot \mathbf{e}_z dz.$$

In the above, \mathbf{e}_x and \mathbf{e}_z are unit vectors in the x direction and z direction, respectively.

2.2. Equivalent Circuit Description

Let $V(s,x)$ in (1) be represented as the difference of two terms, i.e. $V(s,x) = V_f^s(s,x) - V_f^i(s,x)$, where $V_f^s(s,x)$ is the scattered voltage. (1) is reformulated as

$$\frac{d}{dx}V_f^s(s,x) + [R(x) + sL(x)]I(s,x) = V_s(s,x) \quad (3a)$$

$$\frac{d}{dx}I(s,x) + [G(x) + sC(x)]V_f^s(s,x) = 0, \quad (3b)$$

where $V_s(s,x)$ is the distributed voltage source, given by

$$V_s(s,x) = [E_{x,0,h}^i(s) - E_{x,0,0}^i(s)] \cdot \mathbf{e}_x. \quad (4)$$

Fig. 1 shows the modeling of driver circuit under EM wave illumination based on (3). The corresponding circuit model used in noise analysis is shown in Fig. 1(b), where effective driving resistance and parasitic capacitance are used.

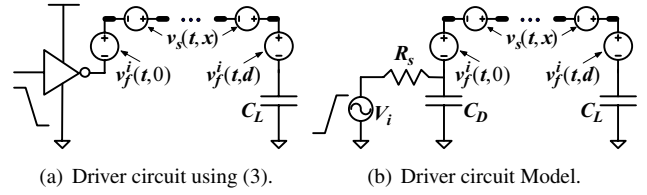


Figure 1. Equivalent driver circuit under EM wave illumination.

2.3. EM Wave Coupling Noise Transfer Functions

Using the principle of linear superposition, the output voltage at loading capacitor C_L is represented as the summation of four voltages in s -domain, i.e.

$$V_{C_L}(s) = V_i(s)H_1(s) + V_f^i(s,0)H_2(s) - V_f^i(s,d)H_3(s) + V_{dist}(s), \quad (5)$$

where $V_{dist}(s)$ denotes the voltage at the output produced by the distributed voltage sources, given by

$$V_{dist}(s) = \int_0^d V_s(s,x)H_{dist}(s,x)dx. \quad (6)$$

Noise transfer functions $H_1(s)$, $H_2(s)$, $H_3(s)$ and $H_{dist}(s,x)$ are given as follows:

$$H_1(s) = \frac{Z_0 Z_L}{H_1^A \cosh \gamma_d + H_1^B \sinh \gamma_d} \quad (7a)$$

$$H_{dist}(s,x) = \frac{Z_L(Z_0 \cosh \gamma_x + Z_D \sinh \gamma_x)}{H_{dist}^A \cosh \gamma_d + H_{dist}^B \sinh \gamma_d} \quad (7b)$$

$$H_2(s) = H_{dist}(s,0), \quad H_3(s) = H_{dist}(s,d) \quad (7c)$$

In the above, $r_d = \gamma \cdot d$, $\gamma_x = \gamma \cdot x$, and

$$\begin{aligned} H_1^A &= Z_0(R_s + Z_L + R_s Y_{CD} Z_L) \\ H_1^B &= Z_0^2(1 + R_s Y_{CD}) + R_s Z_L \\ H_{dist}^A &= Z_0(Z_D + Z_L), \quad H_{dist}^B = Z_0^2 + Z_D Z_L \\ Z_L &= \frac{1}{sC_L}, Y_{CD} = sC_D, Z_D = \frac{1}{1/R_s + sC_D} \end{aligned}$$

Note that $\gamma = \sqrt{(R_0 + sL_0)(G_0 + sC_0)}$, which is the propagation constant of the TL, and $Z_0 = \sqrt{\frac{R_0 + sL_0}{G_0 + sC_0}}$, which is the characteristic impedance of the TL. The PUL (per unit length) parameters of the TL are R_0, L_0, G_0 and C_0 .

3. Handling of Distributed Sources Using Chebyshev Approximation

3.1. Using Chebyshev Approximation

To model voltage $V_{dist}(s)$ generated by those distributed sources, Chebyshev polynomials are used to approximate

(6). $V_s(s, x)H_{dist}(s, x)$ in (6) is represented using Chebyshev polynomials up to order N as:

$$V_s(s, x)H_{dist}(s, x) \approx \sum_{k=0}^N t_k(s)T_k(2x/d - 1). \quad (8)$$

$T_k(\cdot)$ is the k -th order Chebyshev polynomial. The coefficients $t_k(s)$ is given by

$$t_k(s) = \begin{cases} \sum_{j=0}^N \frac{V_s(s, x_j)}{N+1} H_{dist}(s, x_j) & k=0 \\ \sum_{j=0}^N \frac{2V_s(s, x_j)}{N+1} H_{dist}(s, x_j) T_k(y_j) & k>0 \end{cases}$$

and $y_j = \cos \left[\frac{2j+1}{2N+2} \pi \right], x_j = \frac{d}{2}(1+y_j).$ (9)

Based on (6) and (8), Chebyshev approximation of $V_{dist}(s)$ is derived as

$$V_{dist}(s) = \frac{d}{N+1} \sum_{j=0}^N V_s(s, x_j) H_{dist}(s, x_j) f(j, N), \quad (10)$$

where $f(j, N) = 1 + \sum_{k=1}^N \cos \left[\frac{k(2j+1)}{2N+2} \pi \right] \frac{1+\cos k\pi}{1-k^2}.$

3.2. Uniform Plane Wave Illumination Metric

To determine the order of Chebyshev polynomials required in general EM wave coupling situation, the uniform plane wave illumination case is analyzed at first. In this situation, the electrical field of the incident EM wave is in the following form:

$$E_{x,y,z}^i(s) = E_0 \mathbf{e}_f e^{-\frac{s}{v} \mathbf{e}_k \cdot (x,y,z)^T} \quad (11)$$

with $\begin{cases} \mathbf{e}_f = (\cos \beta \cos \theta, \sin \beta, \cos \beta \sin \theta) \\ \mathbf{e}_k = (\cos \alpha \sin \theta - \sin \alpha \sin \beta \cos \theta, \sin \alpha \cos \beta, \\ -\cos \alpha \cos \theta - \sin \alpha \sin \beta \sin \theta) \end{cases}$

v is the phase velocity of the wave in the medium, \mathbf{e}_f is the unit vector representing the direction of electric field, and \mathbf{e}_k is the unit vector representing the EM wave propagation direction. By denoting the projection of E^i in $x-z$ plane as E_{xz}^i , β is then defined as the angle between E^i and E_{xz}^i , θ is defined as the angle between x axis and E_{xz}^i , and α is defined as the angle between propagation direction and vector $E^i \times E_{xz}^i$.

Using the defined uniform plane wave in (11), and using (4), $V_s(s, x)$ is given as

$$V_s(s, x) = E_0 \cos \beta \cos \theta e^{-s \mathbf{e}_{kx}/v} \left(e^{-s \mathbf{e}_{kz}h/v} - 1 \right). \quad (12)$$

\mathbf{e}_{kx} and \mathbf{e}_{kz} are the x and z components of unit vector \mathbf{e}_k respectively. From (6) and (12), the analytical representation

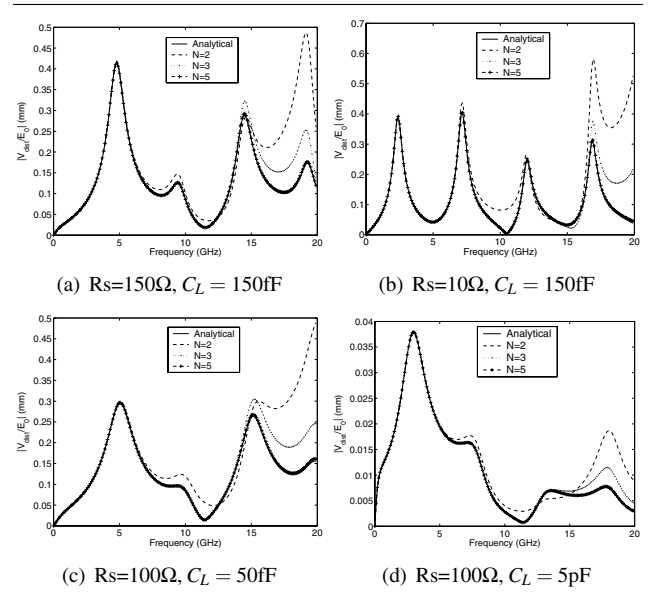


Figure 2. Comparisons between analytical results and chebyshev approximations.

of $V_{dist}(s)$ is derived as

$$V_{dist}(s) = \frac{Z_L E_0 \cos \beta \cos \theta (C^+ - C^-) (e^{-s \mathbf{e}_{kz}h/v} - 1)}{H_{dist}^A \cosh \gamma_d + H_{dist}^B \sinh \gamma_d} \quad (13)$$

where $C^\pm = \frac{(Z_0 \pm Z_D) [e^{\pm (r \mp s \mathbf{e}_{kx}/v)d} - 1]}{2(\gamma \mp s \mathbf{e}_{kx}/v)}$

Fig. 2 compares $|V_{dist}(f)/E_0|$ using Chebyshev approximations based on (10) and using formula (13). For the tested TL circuit ($R_0 = 120 \Omega/m$, $L_0 = 350 \text{ nH/m}$, $C_0 = 120 \text{ pF/m}$, $G_0 = 0$, $d = 15 \text{ mm}$, $C_D = 0$ and $\alpha = \beta = \theta = \frac{\pi}{4}$) with driving and loading conditions varied, the Chebyshev approximation method converges very quickly as N becomes larger. When $N = 2$, the Chebyshev approximations of $V_{dist}(s)$ match the analytical results well up to 6 GHz, the frequency of incident EM wave. The use of $N = 3$ matches the frequency up to 14 GHz, and the use of $N = 5$ matches a frequency range of 20 GHz.

In actual EM wave illumination situation, the incident EM field distribution is arbitrary. Uniform plane wave is employed at first to estimate the required order of Chebyshev approximation. By inserting the PUL parameters of the used interconnection techniques into (13) and (10), N is determined by judging the error between the two calculated results around the maximum EM wave frequency in the actual illumination environment. Next, the actual field values are used to calculate the time-domain noise waveform $V_{dist}(t)$ according to (10).

4. Noise Transfer Function Modeling

Chebyshev approximation is proposed for modeling distributed sources in the last section, and the noise transfer functions at Chebyshev points are required. In this section, a set of concise moment formulas are proposed for the modeling of these noise transfer functions, so that reduced order models can be used to generate noise waveforms efficiently.

4.1. Moments and ROM of $H_1(s)$

$H_1(s)$ is reformulated as

$$H_1(s) = \frac{1}{H_1^C \cosh \gamma_d + H_1^D \frac{\sinh \gamma_d}{\gamma_d}}, \quad (14)$$

where $H_1^C = H_1^A / (Z_0 Z_L) = \sum_{i=0}^{\infty} a_i^C s^i = 1 + s(\tau_s^L + \tau_s^D)$ and

$$\begin{aligned} H_1^D &= H_1^B \gamma_d / (Z_0 Z_L) = \sum_{i=0}^{\infty} a_i^D s^i \\ &= R_s G_d + (\tau_d^L + \tau_s^D) s + (L_d C_L + \tau_d^L \tau_s^D) s^2 + L_d C_L \tau_s^D s^3 \end{aligned}$$

In the above, W_d is the total W for the TL, i.e. $W_d = W_0 \cdot d$, for $W \in \{R, L, G, C\}$, and τ_a^b is a time constant defined as $\tau_a^b = R_a C_b$.

By using the property

$$\cosh x = \sum_{n=0}^{\infty} \frac{x^{2n}}{(2n)!}, \quad \frac{\sinh x}{x} = \sum_{n=0}^{\infty} \frac{x^{2n}}{(2n+1)!} \quad (15)$$

$H_1(s)$ is rewritten as

$$\begin{aligned} H_1(s) &= \frac{1}{\sum_{n=0}^{\infty} (R_d + sL_d)^n (G_d + sC_d)^n \left(\frac{H_1^C}{(2n)!} + \frac{H_1^D}{(2n+1)!} \right)} \\ &= \frac{1}{\sum_{k=0}^{\infty} q_k s^k} \end{aligned} \quad (16)$$

For the most general case that $G_0 = 0$, i.e. $G_d = 0$, to determine the coefficient q_k in (16), the following facts can be utilized:

1. the term s^k can be formed by using $a_i^C s^i$ and $a_i^D s^i$ in H_1^C and H_1^D to multiply a term s^{k-i} from $(R_d + sL_d)^n (sC_d)^n$ in (16).
2. the term s^{k-i} in $(R_d + sL_d)^n (sC_d)^n$ can be formed by letting n goes from $\lceil \frac{k-i}{2} \rceil$ to $k-i$, and using term $(sC_d)^n$ multiply the term s^{k-i-n} in $(R_d + sL_d)^n$.

Hence, q_k is derived as

$$\begin{aligned} q_k &= \sum_{i=0}^{\min(3,k)} \sum_{n=\lceil \frac{k-i}{2} \rceil}^{k-i} \left[\binom{n}{k-i-n} \right. \\ &\quad \cdot C_d^n L_d^{k-i-n} R_d^{2n+i-k} \frac{(2n+1)a_i^C + a_i^D}{(2n+1)!} \left. \right] \end{aligned} \quad (17)$$

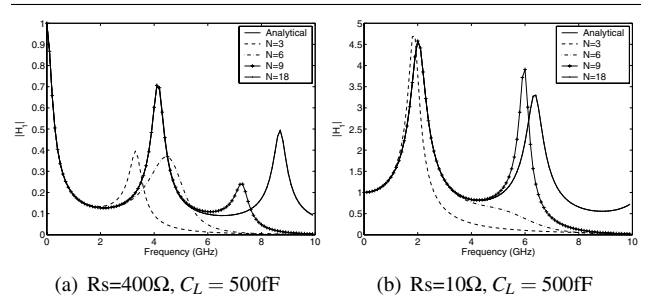


Figure 3. Comparisons between analytical results and Padé approximations of $H_1(s)$.

By (17), the approximation of $H_1(s)$ can be easily made. In one way, the series in the denominator of (16) is truncated to a finite order N , and a rational polynomial in the form of $\frac{1}{\sum_{k=0}^N q_k s^k}$ is used to model $H_1(s)$. The other way is to use general Padé approximation procedure with the order of nominator polynomial chosen in a suitable manner. By (17), the moments of $H_1(s)$ can be generated efficiently for using in the general Padé approximation procedure.

For the completeness of formulation, q_k , when $G_d \neq 0$, is derived from (16) as well. It is given in the following:

$$\begin{aligned} q_k &= \sum_{i=0}^{\min(3,k)} \left\{ \sum_{n=\lceil \frac{k-i}{2} \rceil}^{k-i} \sum_{j=k-i-n}^n \left[\binom{n}{j} \binom{n}{k-i-j} \right. \right. \\ &\quad \cdot R_d^{n-j} L_d^j G_d^{n-k+i+j} C_d^{k-i-j} \frac{(2n+1)a_i^C + a_i^D}{(2n+1)!} \left. \right] \\ &\quad + \sum_{n=k-i}^{\infty} \sum_{j=0}^{k-i} \left[\binom{n}{j} \binom{n}{k-i-j} R_d^{n-j} L_d^j \right. \\ &\quad \cdot G_d^{n-k+i+j} C_d^{k-i-j} \frac{(2n+1)a_i^C + a_i^D}{(2n+1)!} \left. \right] \left. \right\} \end{aligned} \quad (18)$$

Fig. 3 compares $|H_1(f)|$ using analytical formula (7a) and using the truncated order representation of $H_1(s)$, the first approach. Here the TL has the same parameters as in Fig. 2. $C_D = 0$ and the driver's resistance is varied from 400 Ω to 10 Ω . In both of driving conditions, the use of $N = 18$ matches the analytical results in the whole 10 GHz frequency range. The use of $N = 9$ matches up to 5 GHz. When $N = 9$ is chosen, it is suitable to use the general Padé approximation procedure to produce, for example, a 5-pole approximation of $H_1(s)$, relying on the known q_k s.

Using ROM's by matching moments for TL circuits is a convenient approach to address TL effects, for example, [8] presents a set of formulas for such a purpose. However, the limitation in [8] is that low order moments need be approximated sometimes, which may reduce the accuracy of lower order models. The second limitation is that no formulations for higher order moments are available, therefore,

no generalization can be made. This paper, however, gives closed-form moments' representations for the TL driver circuit by (17). The closed-form formulas for arbitrary order transfer function moments are very convenient in deriving ROM's or other analytical metrics for the TL driver circuit.

4.2. Moments and ROM of $H_{dist}(s)$

$H_{dist}(s, x)$ is reformulated as

$$H_{dist}(s, x) = \frac{H_{dist}^E \cosh \gamma_x + H_{dist}^F \frac{\sinh \gamma_x}{\gamma_x}}{H_{dist}^C \cosh \gamma_d + H_{dist}^D \frac{\sinh \gamma_d}{\gamma_d}} = \frac{\sum_{m=0}^{\infty} p_m s^m}{\sum_{k=0}^{\infty} q_k s^k} \quad (19)$$

where

$$\begin{aligned} H_{dist}^C &= (1 + s\tau_s^D) H_{dist}^A / (Z_0 Z_L) = H_1^C \\ H_{dist}^D &= (1 + s\tau_s^D) H_{dist}^B / (Z_0 Z_L) = H_1^D \\ H_{dist}^E &= \sum_{i=0}^{\infty} b_i^E s^i = 1 + s\tau_s^D \\ H_{dist}^F &= \sum_{i=0}^{\infty} b_i^F s^i = R_s G_x + s\tau_s^x \end{aligned}$$

Similarly, W_x is used to denote the lumped parameter for the TL of length x , i.e. $W_x = W_0 x$, for $W \in \{R, L, G, C\}$.

Comparing (16) and (19), the two q_k s are the same. Following the similar way as deriving q_k , the closed-form representation of p_m , for $G_0 = 0$, is derived as

$$p_m = \sum_{i=0}^{\min(1, m)} \sum_{n=\lceil \frac{m-i}{2} \rceil}^{m-i} \left[\binom{n}{m-i-n} \cdot C_x^n L_x^{m-i-n} R_x^{2n+i-m} \frac{(2n+1)b_i^E + b_i^F}{(2n+1)!} \right] \quad (20)$$

Similarly, using W_x to replace W_d in (18), for $W \in \{R, L, G, C\}$, and using b_i^E and b_i^F to replace a_i^C and a_i^D in (18), the representation for p_m , when G_0 is not 0, can be obtained as well.

Fig. 4 shows $|H_{dist}(f)|$ using the analytical formula (7b), and using the truncated series representation in (19). The same TL as in Fig. 2 is used. $C_D = 0$, and the excitation point x is set at the half length point of the TL, i.e. $x = d/2$. For the purpose of demonstration, the numerator polynomial is truncated to $N - 1$, and the denominator polynomial is truncated to N . The results show the correctness of moment function (20). Since p_m and q_k can be easily obtained from the derived formulas, and it is straightforward to obtain the moments for $H_{dist}(s, x)$ from p_m and q_k , the standard Padé approximation procedure can be employed to generate ROM's representing the function, $H_{dist}(s, x)$.

With the closed-form moment functions (17) and (20), either through direct truncation or using the general Padé procedure, rational functions can be formed, and the noise

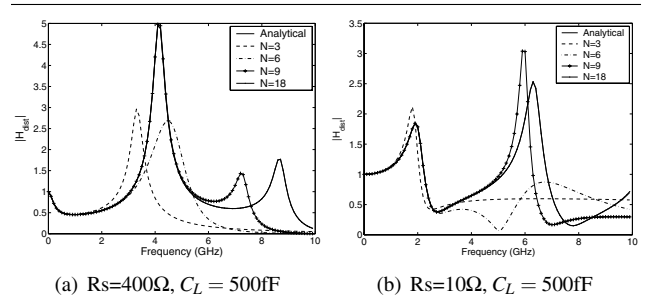


Figure 4. Comparisons between analytical results and Padé approximations of $H_{dist}(s)$.

transfer function can be represented by several poles as below:

$$H(s) = \sum_{i=1}^W \frac{d_i}{s - p_i}, \quad (21)$$

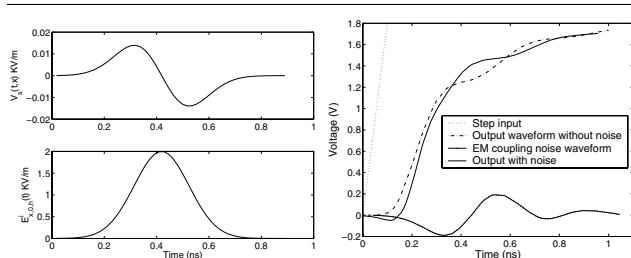
where p_i is the i -th pole obtained from the rational form of noise transfer function, and d_i is the residue. The step response, response to pulse source input, or other type of responses can be obtained conveniently by using (21).

5. Experimental Results

To demonstrate the proposed approach, here the experimental results are presented for a driver circuit, which drives a TL of 20mm length with PUL parameters: $R_0 = 60 \Omega$, $L_0 = 0.6 \mu\text{H}$, and $C_0 = 61 \text{ pF}$. At the other end of the TL, the load is modeled as a 300 fF capacitor. The modeled effective resistance R_s is 200 Ω . The line has a separation of 0.35 mm with the ground. The EM wave illumination situation has a maximum transient electrical field strength of 2 kilovolts per meter. The bandwidth of the incident EM wave is around 10 GHz.

Fig. 5 illustrates the induced EM wave coupling noise in the circuit. The lower graph in Fig. 5(a) shows the transient incident EM field values around the half length point of the TL, which looks like a Gaussian shape waveform and has an amplitude of 2 KV/m and a spread of around 0.4 ns. However, the resulting distributed source $(E_{x,0,h}^i(t) - E_{x,0,0}^i) \cdot \mathbf{e}_x$ has a far less amplitude, which is about 100 times smaller than the amplitude of that location's incident field strength.

Fig. 5(b) shows the results from Hspice simulations only. To model the driver circuit into the Spice netlist, the TL is broken into 20 sections with equal lengths. Then lumped voltage sources $\int_0^{d/20} (E_{x,0,h}^i(t) - E_{x,0,0}^i(t)) \cdot dx$ are used to connect adjacent two sections. In the figure, the noise waveform is only produced by the distributed sources, excluding $V_f^i(t, 0)$ and $V_f^i(t, d)$, since modeling the distributed sources is the major task which raises the difficulty. The noise waveform induced by distributed sources has an amplitude of



(a) EM field stimulus and Dis-tributed Voltage Source (b) EM coupling noise generation at the loading capacitor

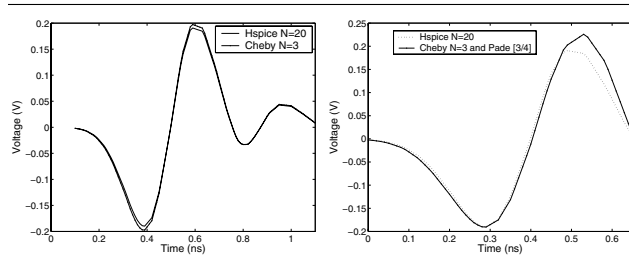
Figure 5. Illustration of Field Stimulus and EM coupling noise.

around 0.2 V in the tested case. It causes around 20 ps delay variation. Since those pulses are as wide as 400 ps, logic faults can also occur if the incident EM wave becomes stronger. For example 8 KV/m field will produce a pulse around 0.4 ns duration and as strong as 0.9 V, which can cause the circuit operating in instable region and finally the logic state may be changed.

Fig. 6 shows the results of the proposed modeling approach compared with Hspice simulation. Fig. 6(a) demonstrates the accuracy of Chebyshev approximation in the modeling of distributed sources. $N = 3$ is chosen as the approximation order, using the uniform plane wave metric and considering the bandwidth of the incident wave is around 10 GHz. In the diagram, the transient noise waveforms using Hspice simulation of twenty-section TL model and Chebyshev approximation with an order of 3 are very close to each other. It shows the effectiveness and accuracy of Chebyshev approximation approach. Fig. 6(b) compares the obtained noise waveforms in the first cycle, by combining Chebyshev expansion and Padé approximation based on the closed-form moment functions, and by using Hspice 20 TLs simulation. Note that in Fig. 6(a), exact transfer functions are used together with Chebyshev approximation. It has demonstrated the correctness of those derived formulas, with which ROM's of various degree of accuracies can be generated quickly.

6. Conclusion

This paper presents a novel modeling technique for considering EM wave coupling noise into conventional VLSI noise analysis flows. The proposed Chebyshev approximation approach for processing the distributed sources is shown as efficient and accurate. The paper gives the closed-form representations of arbitrary order moments for the noise transfer functions. The derived closed-form representations can compute the moments exactly and quickly,



(a) Accuracy of Chebyshev Approx-imation (b) Accuracy of Combining Chebyshev and Padé Approximation

Figure 6. Verification of Modeling Accuracy.

thereby the proposed method will be useful in many design steps such as repeater insertion, timing models, and so on, to produce ROM's or other analytical metrics.

References

- [1] H. Chen and D. Ling. Power supply noise analysis methodology for deep-submicron vlsi chip design. In *Proc. Design Automation Conf.*, pages 638–643, Jun. 1997.
- [2] I. Erdin, A. Dounavis, R. Achar, and M. Nakhla. A spice model for incident field coupling to lossy multiconductor transmission lines. *IEEE Trans. Electromagn. Compat.*, 43(4):485–494, 2001.
- [3] R. Kumar. Interconnect and noise immunity design for the pentium 4 processor. In *Proc. Design Automation Conf.*, pages 938–943, June 2003.
- [4] A. Odabasioglu, M. Celik, and L. Pileggi. prima: passive reduced-order interconnect macromodeling algorithm. *IEEE Trans. Computer-Aided Design*, 17(8):645–654, 1998.
- [5] C. R. Paul. *Analysis of Multiconductor Transmission lines*. Wiley-Interscience Publication, 1994.
- [6] L. Pillage and R. Rohrer. Asymptotic waveform evaluation for timing analysis. *IEEE Trans. Computer-Aided Design*, 9(4):352–366, 1990.
- [7] K. Shepard, V. Narayanan, and R. Rose. Harmony: static noise analysis of deep submicron digital integrated circuits. *IEEE Trans. Computer-Aided Design*, 18(8):1132–1150, Aug. 1999.
- [8] Y. Tanji and H. Asai. Closed-form expressions of distributed rlc interconnects for analysis of on-chip inductance effects. In *Proc. Design Automation Conf.*, pages 810–813, June 2004.
- [9] S. Tkatchenko, F. Rachidi, and M. Ianoz. High-frequency electromagnetic field coupling to long terminated lines. *IEEE Trans. Electromagn. Compat.*, 43(2):117–129, May. 2001.
- [10] J. M. Wang, E. S. Kuh, and Q. Yu. The chebyshev expansion based passive model for distributed interconnect networks. In *Proc. Int. Conf. Computer-Aided Design*, pages 370–375, Nov. 1999.
- [11] H. Zhou. Timing analysis with crosstalk is a fixpoint on a complete lattice. *IEEE Trans. Computer-Aided Design*, 22(9):1261–1269, Sept. 2003.